Suppression of Tumorigenesis and Metastasis of Hepatocellular Carcinoma by shRNA interference targeting on homeoprotein Six1

Kevin T.P. NG

Terence K.W. Lee

Qiao Cheng

Jana Y.H. Wo

Chris K.W. Sun

Dong-Yong Guo

Zophia X. Lim

Chung-Mau Lo

Ronnie T.P. Poon

Sheung-Tat Fan

Kwan Man

Department of Surgery and Centre for Cancer Research, LKS Faculty of Medicine, The University of Hong Kong

Corresponding author
Dr. K. Man
Department of Surgery and Centre for Cancer Research
The University of Hong Kong, Pokfulam
L9-55, Faculty of Medicine Building
21 Sassoon Road
Hong Kong, China
Tel: 852-28199646
Fax: 852-28199634

E-mail: kwanman@hkucc.hku.hk

Short title: The role of homeoprotein Six1 in hepatocellular carcinoma

Key words: Hepatocellular carcinoma, homeoprotein Six1, short hairpin RNA (shRNA) interference, metastasis, cDNA microarray.

Abbreviations: HCC, hepatocellular carcinoma; pTNM, pathologic tumor metastasis; shRNA, short hairpin RNA; sqRT-PCR, semi-quantitative RT-PCR.

Journal category: Cancer Cell Biology

Novelty and impact: We firstly demonstrated that suppression of homeoprotein Six1 led to *in vitro* and *in vivo* decreases of tumorigenicity and metastatic ability of hepatocellular carcinoma (HCC). We believe that these findings are indispensible, in part, for understanding the carcinogenesis and metastasis of HCC and for development of therapeutic strategy for treatment of HCC.

Abstract

We previously demonstrated that overexpression of homeoprotein Six1 in hepatocellular carcinoma (HCC) patients is associated with venous infiltration, advanced pathologic tumor metastasis (pTNM) stage and poor overall survival rate [1]. In this study, short hairpin RNA (shRNA) interference approach was used to suppress the expression of Six1 in a metastatic HCC cell line MHCC97L. Stable transfectant MHCC97L-shSix1 carrying Six1 specific shRNA plasmid was established to downregulate Six1 expression to about 40% compared to MHCC97L-Control. *In vitro* functional assays demonstrated that the growth rate and proliferation ability of MHCC97L-shSix1 cells were markedly decreased. Moreover, significant decrease of cell motility and invasiveness were observed in MHCC97L–shSix1 cells. Data from *in vivo* xenograft tumorigenesis model demonstrated that the size of tumor in MHCC97L-shSix1 group was dramatically reduced. Experimental and spontaneous metastasis models indicated that targeting Six1 suppression noticeably reduced the pulmonary metastasis in MHCC97L-shSix1 group. To identify Six1-regulated targets, cDNA microarray was employed to compare the expression profiles of MHCC97L-Control and MHCC97L-shSix1 cells. Twenty-eight down-regulated and 24 up-regulated genes with known functions were identified in MHCC97L-shSix1. The functions of these target genes are involved in diverse biological activities. Our data suggest that Six1 may be involved in regulation of proliferation and invasiveness of HCC; thus targeting suppression of Six1 is a viable option for treating HCC patients.

Introduction

Hepatocellular carcinoma (HCC) is one of the most malignant tumors in the world, causing more than 600 000 deaths per year [2]. Surgical treatments in terms of hepatic resection and orthotopic liver transplantation are frontline treatments for HCC, but the long-term disease-free survival remains unsatisfactory [3, 4]. Tumor recurrence and metastases are the major causes of death in HCC patients after surgical treatments [5, 6], indicating the necessity of developing new therapeutic strategies targeting at tumor recurrence and metastases in HCC. Up to now, the molecular mechanisms of HCC metastasis remain unclear; hence identification and characterization of novel metastasis-associated genes are indispensable for development of effective treatment of HCC patients.

Homeoprotein Six1 belongs to a subfamily of the Six family of homeodomain-containing transcription factors that shares a lysine within the DNA-binding helix of the homeodomain [7, 8]. Six1, located at 14q23 of the chromosome is involved in early developments of diverse organs such as the brain, ear, eye, muscle and kidney [8-12]. Alteration of Six1 expression takes place in human breast cancer, Wilms' cancer, ovarian cancer and rhabdomyosarcoma, indicating its possible contributions in the tumorigenicity of different cancers [13-16]. Six1 is also regarded as an important metastatic regulator in cancers. For example, overexpression of Six1 occurs in a large percentage of primary cancers, and strongly correlates with breast lesions [15]. Six1 elevated in breast cancer promotes progression of breast cancer [17]. Six1 also plays a substantial role in regulating the metastatic ability of rhabdomyosarcoma [13]. The impact of Six1 on promoting tumorigenesis and metastasis of multiple cancers therefore impelled us to study the property of Six1 in HCC. We previously found that Six1 protein is specifically overexpressed in tumor tissues rather than non-tumor tissues of HCC patients. Overexpression of Six1 protein is significantly associated with venous infiltration, advanced

pathologic tumor metastasis (pTNM) stage and poor overall survival of HCC patients after surgical resection [1]. Also, *in vitro* gene expression analysis found that Six1 protein is specifically expressed in metastatic HCC cells but not in non-metastatic HCC cells [1].

In the present study, we suppressed the expression of Six1 in a metastatic HCC cell using short hairpin RNA (shRNA) interference technique to study the possible roles of Six1 in proliferative and metastatic abilities of HCC through *in vitro* and *in vivo* functional assays. Furthermore, cDNA microarray approach was employed to identify possible downstream targets of Six1 shedding some light on the regulation mechanism via in HCC.

Material and methods

Cell lines

A human metastatic HCC cell line MHCC97L was a gift from Liver Cancer Institute & Zhongshan Hospital of Fudan University, Shanghai, People of Republic of China [18]. The cell was cultured in DMEM high glucose medium (Gibco) with 10% fetal bovine serum (FBS, Gibco) and 1% penicilium and streptomycin in a 37^{o}C incubator supplied with 5% CO_2.

Establishment of stable shRNA transfectant

Oligonucleotide (CCAGCTCAGAAGAGGAATT) targeting Six1 gene was cloned into pGE-1 shRNA expression vector (Stratagene) according to manufactory's instruction, designated pGE-1-shSix1. The sequence of pGE-1-shSix1 was confirmed by both enzymatic cutting with *BamHI* and *XbaI* and sequencing reaction using 5' sequencing primer: 5' CGTCGATTTTTGTGATGCTCGTCAG 3'. Control shRNA vector (Stratagene) and pGE-1-shSix1 were transfected into MHCC97L and under G418 selection for 2 weeks. MHCC97L-shSix and MHCC97L-Control represent cell lines stably transfected with pGE-1-shSix1 and control shRNA vector respectively.

Reverse transcription-polymerase chain reaction (RT-PCR)

Total RNA was extracted by using RNeasy Mini Kit (Qiagen). Each cDNA was synthesized from 1μg of total RNA using High capacity cDNA Kit (Applied BioSystems) under the condition of 25^{o}C for 5 minutes following by 37^{o}C for 2 hours. PCR reaction for Six1 gene was performed using Taq PCR kit (Promega) under the following PCR cycles: 95^{o}C for 5 minute, 30 cycles of 95^{o}C for 1 minute, 57^{o}C for 1 minute and 72^{o}C for 1 minute. Amplification of 18S ribosomal RNA was used as an internal control. PCR products were visualized by 2% agarose gel electrophoresis stained with ethidium bromide. Primers sets

used were as follows: for Six1, sense AAG GAG AAG TCG AGG GGT GT, antisense TGC TTG TTG GAG GAG GAG TT; for 18S ribosomal RNA, sense CTC TTA GCT GAG TGT CCC GC, antisense. CTG ATC GTC TTC GAA CCT CC.

Western blot analysis

Proteins were extracted by 1X Lysis Buffer (Cell Signaling Technology). Protein extracts were separated by 12% SDS-PAGE and transferred to PDMF membrane (Millipore). After blocking with 5% non-fat milk for 1 hour, antibody, appropriately diluted, was hybridised with the membrane at 4^{o}C over night. The membrane was washed 3 times with TBS/T each for 10 minutes and incubated with secondary antibody for 1 hour at room temperature. Protein signal was detected by ECL Plus system (GE Healthcare). Antibodies Six1 and β-Actin were purchased from Santa Cruz Biotechnology.

Ultrastructural examination by scanning electron microscopy

Cells grown on the cover-slips were fixed with 2.5% glutaraldehyde in 0.1 M sodium cacodylate-HCL buffer, pH 7.4, quenched with 0.1 M sucrose/cacodylate solution, washed in cacodylate buffer, and then fixed with 1% OsO4 in cacodylate buffer. After cacodylate buffer wash, the samples were dehydrated through a graded series of ethanol washes, followed by critical point drying using a Bal-Tec CPD 030 critical point dryer (Bal-Tec AG, Liechtenstein). Lastly, the samples were sputter-coated with a layer of gold (Bal-Tec SCD005 Sputter Coater, Bal-Tec AG) and visualized using Leica Cambridge Stereoscan 440 SEM at an accelerating voltage of 12 kV [19].

Cell proliferation assay

One thousand of cells were seeded on 96-well plate and incubated in normal condition.

Cells were analysed by (3-(4,5-Dimethylthiazol-2-yl)-2,5-diphenyltetrazolium bromide (MTT) (GE Healthcare) assay at 24-hour interval for 5 days. After incubation for 24 hours, cells were treated with 100µl of 5mg/ml of MTT solution for 4 hours at 37^{o}C until crystals were formed. MTT solution was removed from each well and the crystals were dissolved with 100µl of DMSO. Color intensity was measured by Microplate Reader (Model 680, Bio-Rad) at 570nm. Each experiment consisted of five replications and at least four individual experiments were carried out

Colony formation assay

Five hundreds of cells were seeded onto 6-well plate and incubated in normal condition. After 2 weeks cultivation, cells were fixed by ice-cold methanol for 30 minutes and stained by Crystal violet for 10 minutes. Colonies (more than 50 cells) were counted directly on the plate. Statistical significant was calculated from each four independent experiments.

Cell cycle analysis

Cells ($3x10^5$) were seeded onto 6-well plate and synchronized in G_0 by serum starvation for 3 days (DMEM without serum). Complete medium (DMEM plus 10% FBS) was replaced to stimulate the cell proliferation for the following 48 hours. At time 0, 24 and 48 hours interval, cells were trypsinized and fixed with 75% ice-cold ethanol for one hour. After 3 times PBS washing, cells were stained with 1µg/ml of propidium iodide (PI) and 0.5µg/ml of RNase A at 37^{o}C for 30 minutes. Cell cycle was analysed by flow cytometry. Each experiment was analysed in triplicate and at least three independent experiments were performed.

Wound healing assay

Cells ($8x10^5$) were seeded onto 24-well plate and incubated for 24 hours. Prior to

experiment, cells were treated with 10μg/ml mitomycin C (Sigma) for 3 hours. A straight-line-wound was made by scraping a 20μl-pipette tip across the cell monolayer. Cells were rinse with PBS and cultured in DMEM supplemented with varying concentration of FBS (1%, 5% and 10%) for 24 hours. The movement of cells towards the wound was captured under 100X magnification.

Migration assay

Migration ability of the cells were analysed by Polyethyleneterephthalate (PET)-based migration chamber with 8μm porosity (BD Labware, NJ). $5x10^4$ cells were suspended in 500 μl of serum-free DMEM and seeded into the migration chamber. The migration chamber was placed into a 24-well plate with 500μl of DMEM containing 10% FBS and incubated at 37^oC with 5% CO_2. After 24 hours of incubation, cells on the upper surface of the chamber were scrapped out by a cotton swab. Cells migrated through the chamber were stained by hematoxylin and eosin (H & E) and subsequently counted under the microscope. At least three independent experiments were performed.

Collagen type I assay

Five microliters of cells ($3x10^4$ cells/ml) were mixed with 50μl of ice-cold rat tail collagen, type I (4.4mg/ml, BD Biosciences, MA). The mixture was plated as droplets in a 6-well plate until solidified; three droplets were made for each sample. The droplets in the plate were covered with DMEM medium containing 10% FBS and cultured for one week. Cell morphology was observed under microscope and captured under 400X magnification. One hundred colonies for each sample were counted and percentage of colonies that showing elongated morphology was calculated.

Immunofluorescent staining of F-actin

Each of 3000 cells of MHCC97L-Control and MHCC97L-shSix1 were cultivated overnight on 8mm diameter Hydrophobic Printed Slide (Electron Microscopy Sciences). The cells were subjected for serum-starvation for 2 days. Induction of F-actin was performed by incubating the cells with 0.01μM lysophosphatidic acid (LPA) for 1 hour. The cells were washed with PBS buffer, fixed with 4% formaldehyde dissolved in PBS for 10 minutes at room temperature and permeabilized for 15 minutes with 0.1% Triton X-100. The cells were blocked with 1% bovine serum albumin in PBS for 30 minutes and then incubated with 1μg/ml FITC-phalloidin (Sigma-Aldrich) at 37^{o}C overnight. After 3 washes in PBS, the cells were stained with DAPI at room temperature for 10 minutes. The cells were washed 3 times with PBS and mounted with FluorSave Reagent (Calbiochem). The slides were analyzed by an image analysis system (Eclipse E600, Nikon).

In vivo tumorigenicity model

Cells ($2x10^6$) were suspended in 150μl of saline and subcutaneously injected into each nude mouse. The tumor size and body weight were measured for every 5 days. After 6 weeks, the mice were sacrificed and the tumors were harvested for further analysis. Six mice were recruited for each of the experimental group. Volume of the tumor was calculated as follows: tumor volume (cm^3) = 1/2 x larger size x smaller size^2.

In vivo experimental and spontaneous metastasis models

In vivo experimental metastasis model was established by injection of $2x10^6$ cells suspended in 100μl of saline into the tail vein of nude mice. The *in vivo* spontaneous metastasis model was established in an orthotopic nude mice liver cancer model. Firstly, $2x10^6$ cells were subcutaneously injected into the left flank of the nude mice. The subcutaneous tumor tissues were then harvested once the tumor size reached $1cm^3$. It was cut

into about 1mm^3 pieces and orthotopically implanted into the left lobes of the livers of another groups of nude mice [20]. All mice were fed in standard condition with weight monitoring and sacrificed after 6-week incubation. Volume of the tumor was calculated as follows: tumor volume (cm^3) = length x width x thickness. Liver and lung tissues were fixed by 10% formalin solution and subsequently analyzed by H & E staining.

cDNA microarray analysis

Genome-wide expression profile was analyzed by gene chip system Human U133 Plus 2.0 (Affymetrix Inc. Santa Clara, CA). RNA quality control, sample labeling, GeneChip hybridization and data acquisition were performed at the Genome Research Centre, The University of Hong Kong. Total RNA was extracted from cells using RNeasy mini Kit (Qiagen). The quality of total RNA was checked by the Agilent 2100 bioanalyzer. The RNA was then amplified and labeled with MessageAmp II-Biotin Enchanced Single Round aRNA Amplification Kit (Ambion Inc., Texas). In brief, double-stranded cDNA was generated by reverse transcription from 1ug of total RNA with an oligo(dT) primer bearing a T7 promotor. The double strand cDNA was used as a template for *in vitro* transcription to generate biotin-labeled cRNA. After fragmentation, 15ug of cRNA was hybridized to the GeneChip array for 16 hours. The GeneChips were washed and stained using the GeneChip Fluidics Station 400 (Affymetrix Inc.) and then scanned with the GeneChip Scanner 3000 (Affymetrix Inc.). The experiment was performed twice. To compare the gene expression pattern between MHCC97L-Control and MHCC97L-shSix1, hybridization intensity between these 2 samples was normalized by Affymetrix global scaling method (Affymetrix Inc.). Genes with 2-fold difference, either increased or decreased, were selected for further confirmation by SYBR Green real-time PCR.

Confirmation of cDNA microarray data by SYBR green real-time RT-PCR

Each 1μg of total RNA from MHCC97L-Control and MHCC97L-shSix1 cell lines was used to synthesize 22μl of cDNA using the High capacity cDNA Kit (Applied Biosystems, Foster City, CA). PCR analysis of each of the target gene was carried out in the following PCR mixture: 1μl of cDNA, 10μl of 2X Power SYBR Green PCR Master Mix (Applied Biosystems), 0.1μl of 10mM forward primer, 0.1μl of reverse primer and 8.8μl of distilled water. Primers for target genes are listed in Table I. Real-time PCR was carried out in a 7700 Sequence Detection Instrument (Applied Biosystems) using the following thermal cycling profile: 95^{o}C 1 minute, followed by 40 cycles of amplification (95^{o}C 15 seconds, 60^{o}C 4 minutes). Analysis of dissociation curve for each pair of primers was conducted to examine the specificity of each PCR product.

Statistical analysis

Statistical analysis was carried out using SPSS 16.0 for Windows (SPSS Inc., IL). Two-tailed Student's t test was used for analysis of continuous variables. $P < 0.05$ was considered to be statistically significant.

Results

Suppression of Six1 expression by shRNA

MHCC97L, a HCC cell line with metastatic potential to lung [18], overexpresses Six1 gene compared with other non-metastatic HCC cells [1]. To investigate the role of Six1 in HCC metastasis, MHCC97L was transfected with DNA based Six1-specific shRNA plasmid (pGE-1-shSix1) and control plasmid (pGE-1-Control). The expression level of Six1 gene was suppressed by more than 2-folds in MHCC97L-shSix1 cell, both in mRNA (Fig. 1*a*) and protein (Fig. 1*b*) levels, compared to MHCC97L-control cell. Microscopically, the morphology of MHCC97L-shSix1 was changed to a rounder and more compressed shape compared with MHCC97L-Control (Fig. 1*c*). Under electron microscope (EM) analysis, MHCC97L-shSix1 displayed less numbers of extracellular "hair-like" connection fibres (lamellipodia formation) compared to MHCC97L-Control (Fig. 1*d*).

Effect on cell proliferation and colony formation

To investigate the effect of Six1 suppression on cell growth, MTT assay was employed to analyse the growth rate of MHCC97L-shSix1 and MHCC97L-Control for 5 days. Compared with MHCC97L-Control, MHCC97L-shSix1 exhibited slower growth rate and reached 2-fold difference on day 4 (Fig. 2*a*). Statistical analysis, by t-test, showed significant difference between 2 groups on day 2, 3, 4 and 5 ($P < 0.01$). Moreover, the number of colony formed in MHCC97L-shSix1 were significantly less than that in MHCC97L-Control (23 vs 108 in average, p=0.000, Fig. 2*b*).

Effect on cell cycle

To examine the effect of Six1 suppression on the cell cycle, DNA content of MHCC97L-shSix1 and MHCC97L-Control was analyzed by FACS using propidium iodide

(PI) staining. The cells were subjected to serum starvation for 3 days for synchronization of the cells in G_0 phase, followed by re-supplementation of 10% serum for 2 days. The percentage of G2/M phase of MHCC97L-shSix1 were consistently higher than that of MHCC97L-Control on day 0, 1 and 2 (Fig. 3*a*). These results demonstrated that suppression of Six1 expression leads to a delay in G2/M transition (Fig. 3*b*).

Effect on cell motility and invasion

To investigate the effect of Six1 suppression on cell motility, three common methods including wound healing assay, migration assay and collagen type I invasion assay were performed on MHCC97L-Control and MHCC97L-shSix1 cells. Wound healing assay at 24 hours after the creation of straight wound line showed that the wound in MHCC97L-Control almost recovered while the wound in MHCC97L-shSix1exhibitted only slight improvement (Fig. 4*a*). It was estimated that the wound-healing ability of MHCC97L-shSix1 was at least 2-fold less than that of the MHCC97L-Control after 24 hours. Consistent results were observed at different serum concentrations. Migration assay showed that the number of migrated MHCC97L-shSix1 cells after 24 hours were about 50% less than that of MHCC97L-Control (69 vs 143 migrated cells in average, P=0.000, Fig. 4*b*). Using three dimensional collagen type I invasion assay, it was found that less number of MHCC97L-shSix1 cells grew inside the collagen gel and exhibited an elongated or scattered patterns compared with MHCC97L-Control (P=0.000, Fig. 4*c*). The above results demonstrated that down-regulation of Six1 gene suppressed the motility and invasiveness of metastatic HCC cells.

Effect on distribution of F-actin

Phalloidin staining of MHCC97L-Control after LPA stimulation showed that F-actin was evenly distributed all over the cells (Fig. 5). While in MHCC97L-shSix1, F-actin expression

was suppressed leading to decrease in stress fiber polymerization. This data demonstrated that suppression of Six1 expression decreases F-actin polymerization

Effect on in vivo tumorigenicity

The tumor growth rate was significantly delayed in MHCC97L-shSix1 group compared to MHCC97L-Control group at all time points (Figs. 6*a* and 6*b*). At day 30, the tumor size in MHCC97L-Control group was about 5-fold of the tumor size in MHCC97L-shSix1 group ($1.71cm^3$ vs $0.36cm^3$ in average, p=0.000). The body weight in these two groups was similar (data not shown). Western blot analysis of subcutaneous xenografts showed that the level of Six1 protein in MHCC97L-shSix1 xenograft was also lower than in MHCC97L-Control xenograft (Fig. 6*c*).

Effect on in vivo metastasis

We performed experimental and spontaneous metastasis models to evaluate the effect of Six1 suppression on metastatic behaviours of MHCC97L cell line. For the experimental metastasis model, 6 weeks after inoculation, 3 of 7 (42.9%) mice were found to have pulmonary metastasis by H&E staining in MHCC97L-Control group (Fig. 7*a*), while there is no pulmonary metastasis in MHCC97L-shSix1 group. No liver tumor was found in both groups (Table II). However, the difference between these two groups was statistically insignificant (Table II).

For the spontaneous metastasis model, 6 weeks after the implantation, it was found that less liver tumor formed in MHCC97L-shSix1 group (6 of 8, 75%) compared to that of the MHCC97L-Control group (8/8, 100%). Moreover, the average size of liver tumor in MHCC97L-shSix1 group was noticeably smaller than that of the MHCC97L-Control group (Fig. 7*b* and Table II). Furthermore, the aggressive phenotype of tumor was attenuated in

MHCC97L-shSix1 group compared to MHCC97L-Control group (Fig. 7*b*). Lastly, H & E staining of lung section (Fig. 7*b*) revealed that more than 60% (5 of 8) of mice in MHCC97L-Control group showed pulmonary metastasis while no pulmonary metastasis case was developed in MHCC97L-shSix1 group (Table II). Statistical analysis indicated that both tumor volume (p=0.000) and metastasis potential (p=0.026) in MHCC97L-shSix1 group were significantly reduced compared to MHCC97L-Control group (Table II).

Identification of downstream targets of Six1

To find out the genes under the regulation of Six1, gene expression profiles of MHCC97L-shSix1 were compared with MHCC97L-Control using cDNA microarray analysis. A total of 61 down-regulated and 59 up-regulated differential targets were found in MHCC97L-shSix1 compared to that in MHCC97L-Control. After screening out those unknown genes and EST sequences, a total of 28 down-regulated and 24 up-regulated genes with known functions were identified (Tables III and IV). A summary for down-regulated and up-regulated genes was generated based on their functions (Fig. 8).

To validate the cDNA microarray results, 15 either down-regulated or up-regulated genes that have higher fold changes among samples were selected and confirmed by SYBR green real-time semi-quantitative RT-PCR (sqRT-PCR). Dissociation curve for each gene was tested to make sure that only a specific PCR product indicated by production of a single peak was generated for each pair of primers (data not showed). Otherwise, new pairs of primers were redesigned and retested. The Ct value for each gene was normalized with the Ct value of 18S primers. For down regulated genes, most of the results from sqRT-PCR were consistent with the findings from cDNA microarray analysis (Table III). For up-regulated genes, sqRT-PCR results showed higher fold changes than the microarray analysis (Table IV).

Genes differentially expressed upon suppression of Six1 gene were found to be involved in

diverse physiological roles. Among those down-regulated genes, most of the genes were involved in signal transduction, protein trafficking and metabolism (Fig. 8). Moreover, several oncogenes such as *YWHAH*, *CD46*, *CRKII* and *ADAM 10* were down-regulated. While up-regulation of genes involved in transcription regulation, cell growth, transport, immunity and signal transduction (Fig. 8).

Discussion

Several lines of evidence suggest that Six1 is deregulated in various mammalian cancers and overexpression of Six1 lead to an increase of malignancy of tumors subsequently causing higher mortality rate of cancer patients [13, 15, 16]. In HCC, overexpression of Six1 protein is significantly correlated with advanced pTNM stage, venous infiltration and poor overall survival [1]. To further investigate the possible role of Six1 in HCC, we employed shRNA technology to suppress the expression of Six1 gene in a metastatic HCC cell line MHCC97L which overexpresses Six1 protein compared with other non-metastatic HCC cell lines [1]. We generated stable clone (MHCC97L-shSix1) in which Six1 expression was suppressed over 50% in both mRNA and protein levels compared to MHCC97L-Control. *In vitro* assays showed that suppression of Six1 expression significantly reduced the growth rate and the ability of forming colonies of MHCC97L, suggesting that Six1 may play an essential role on tumor proliferation. *In vivo* xenograft tumorigenesis model also supported that inhibition of Six1 expression hindered the growth rate of HCC in nude mice. In breast cancer, overexpression of Six1 promotes tumorigenesis and progressiveness of the tumor by targeting cyclin A1 expression [17]. Moreover, overexpression of Six1 in ovarian cancer promotes the proliferative phenotype of the tumor cell [16]. All these evidences suggested that Six1 may participate in oncogenic regulation in multiple cancers.

Deregulation of cell cycle control is one of the characteristics of cancers. Abrogation of G2/M phase arrest induced by DNA damage is a mechanism of cancer cells to resist therapies such as radiation and chemotherapy. Six1 has been identified in the late S phase in breast cancer and its overexpression can abrogate DNA damage-induced G2 cell cycle arrest [15]. In our present study, cell cycle analysis showed that suppression of Six1 expression in MHCC97L resulted in a delay in G2/M transition suggesting that Six1 may function in G2/M phase regulation in HCC. An arrest in G2/M phase can disrupt cell cycle progression and can

be attributed to the observed decrease in growth rate of MHCC9L-shSix1 cells with respect to MHCC97L-Control cells. The role of Six1 on G2/M phase regulation of HCC is thus beneficial to understand the abnormal progression of cell cycle and chemoresistance of HCC. The mechanism of Six1 in G2/M regulation and the relationship with cell cycle regulators in HCC remains to be determined.

MHCC97L is a metastatic HCC cell line which can metastasize to lung from liver [21]. Our data showed that suppression of Six1 expression in this cell line resulted in inhibition of its *in vitro* metastatic activities including wound-healing, migration and invasion abilities. Decreases in lamellipodia formation on the cell surface and intracellular stress fiber polymerization were observed in MHCC97L-shSix1 indicating that suppression of Six1 expression could reduce the motility of the cell. Furthermore, a significant suppression of lung metastasis was observed in MHCC97L-shSix1 group in the *in vivo* spontaneous metastasis model. The *in vivo* metastasis rate of MHCC9L-Control in spontaneous metastasis model was 62.5% in our study (Table II) which is higher than that of the original MHCC97L (40%) claimed by Li *et al*, [21]. This may be due to accumulative genetic changes leading to increased metastatic potential of this cell line. Altogether, these results implied that the function of Six1 may be linked to metastatic ability of HCC. Therefore alteration of Six1 expression may influence certain step(s) of the metastatic pathway of HCC. In rhabdomyosarcoma, *in vitro* and *in vivo* experiments indicated that changes in Six1 expression can alter the metastatic potential of rhabdomyosarcoma cell lines. Forced up-regulation of Six1 overexpression can increase the metastatic potentials of the poorly metastatic rhabdomyosarcoma cell lines while suppression of Six1 expression can reduce the metastatic potential of the highly metastatic rhabdomyosarcoma cell line [13]. Metastasis is one of the major causes of death in HCC patients due to malignant status of the tumor and no effective treatment for these patients. An increasing number of metastasis-associated genes

were identified in HCC in recent years [22, 23]. Unfortunately, the regulation mechanism of metastasis of HCC is still not very clear even to this date. . Therefore, identification and characterization of novel metastasis-associated genes are crucial for understanding its possible mechanism and ultimate, for the development of an effective therapeutic strategy. Taken together, our results demonstrated that Six1 is undoubtedly involved in the progression and metastasis of HCC. Suppression of Six1 expression successfully hindered both tumorigenesis and metastasis of HCC suggested its potential therapeutic value in treatment of HCC.

Six1 can activate several genes during development and more importantly, in cancers [24]. Identification of downstream targets of Six1 in HCC would provide better understanding on its regulation mechanism in HCC. With this in mind, cDNA microarray analysis was performed to identify differential genes in MHCC97-shSix1 compared to MHCC97L-Control. A total 120 differential genes were identified and finally 28 down-regulated and 24 up-regulated genes with known functions were obtained. These differential genes function involved in diverse biological activities such as signaling regulation, protein trafficking, transcription regulation and growth control, revealing that Six1 can activate multiple genes in HCC. In other cancers, Six1 can activate several oncogenes, such as Cyclin A1 in breast and ovarian cancers [16, 17] and c-Myc, Cyclin D1 as well as ezrin in rhabdomyosarcoma [25]. Several tumor-associated genes were found to down-regulated in MHCC97L-shSix1 including *YWHAH* (or *14-3-3 eta*), *CD46*, *CRKII* and *ADAM 10* [26-29], indicating that Six1 may regulate the expression of these oncogenes in HCC. The downstream targets of Six1 identified in HCC were different from other cancers suggested that the regulation mechanism of Six1 in HCC may be different from other cancers. Six1 may activate the expression of various genes involved in different biological functions that may probably take part in carcinogenesis and metastasis of HCC. The functions of these differential genes and their relationship with Six1 are needed to be further characterized.

Our study demonstrated that suppression of Six1 led to decreases of tumorigenicity and metastatic ability of HCC suggesting its important therapeutic implications for future drug development and treatment of HCC.

Figure legends

FIGURE 1 - (a) RT-PCR and (b) Western blot analyses of Six1 gene among MHCC97L, MHCC97L-Control and MHCC97L-shSix1 cells.. Ribosomal RNA (18S) and beta-actin protein were use as internal control for RT-PCR and Western blot respectively. (c) Microscopic and (d) Scanning electron microscope examination of the morphologies of MHCC97L-Control and MHCC97L-shSix1 cells.

FIGURE 2 - Proliferation characteristics of MHCC97L-Control and MHCC97L-shSix1 cells. (a) MTT assay of cells. (b) Colony formation assay. *, $p < 0.01$.

FIGURE 3 - Cell cycle analysis of MHCC97L-Control and MHCC97L-shSix1 cells for 2 days. (a) Histogram of cell cycles. (b) Comparison of percentage of G_2M phase between MHCC97L-Control and MHCC97L-shSix1.

FIGURE 4 - Cell motility and invasion assays of MHCC97L-Control and MHCC97L-shSix1 cells. (a) Wound healing assay after 24 hours in different serum concentration. Arrows indicate the gap between wound. (b) Migration assay after 24 hours. (c) Collagen type I assay after 1 week. *, $P < 0.01$.

FIGURE 5 - F-actin staining of MHCC97L-Control and MHCC97L-shSix1 cells.

FIGURE 6 - Xenograft tumorigenesity model between MHCC97L-Control and MHCC97L-shSix1 groups. (a) Representative subcutaneous xenografts generated in mice after 30-day inoculation. (b) Tumor size of subcutaneous xenografts measured with 5-day

interval. *, $p < 0.01$. (c) Western blot analysis of Six1 protein level between the subcutaneous tumor xenografts from MHCC97L-Control and MHCC97L-shSix1 groups.

FIGURE 7 - (a) H & E staining of formalin fixed lung tissues from MHCC97L-Control and MHCC97L-shSix1 groups in experimental metastasis model. (b) Representative liver xenografts, H & E staining of liver tissues and lung tissues of MHCC97L-Control and MHCC97L-shSix1 groups in spontaneous metastasis model. Arrows indicate the formation of tumors in lung tissues.

FIGURE 8 - Summary of differential genes in MHCC97L-shSix1 comparing with MHCC97L-Control. Number (s) followed each category indicates the number of genes found.

References

1. Ng KT, Man K, Sun CK, Lee TK, Poon RT, Lo CM, Fan ST. Clinicopathological significance of homeoprotein Six1 in hepatocellular carcinoma. British journal of cancer 2006;95:1050-5.

2. Bosch FX, Ribes J, Diaz M, Cleries R. Primary liver cancer: worldwide incidence and trends. Gastroenterology 2004;127:S5-S16.

3. Poon RT, Fan ST. Hepatectomy for hepatocellular carcinoma: patient selection and postoperative outcome. Liver Transpl 2004;10:S39-45.

4. Lo CM, Fan ST. Liver transplantation for hepatocellular carcinoma. Br J Surg 2004;91:131-3.

5. Llovet JM, Schwartz M, Mazzaferro V. Resection and liver transplantation for hepatocellular carcinoma. Semin Liver Dis 2005;25:181-200.

6. Tung-Ping Poon R, Fan ST, Wong J. Risk factors, prevention, and management of postoperative recurrence after resection of hepatocellular carcinoma. Ann Surg 2000;232:10-24.

7. Oliver G, Wehr R, Jenkins NA, Copeland NG, Cheyette BN, Hartenstein V, Zipursky SL, Gruss P. Homeobox genes and connective tissue patterning. Development (Cambridge, England) 1995;121:693-705.

8. Kumar JP. The sine oculis homeobox (SIX) family of transcription factors as regulators of development and disease. Cell Mol Life Sci 2009;66:565-83.

9. Laclef C, Souil E, Demignon J, Maire P. Thymus, kidney and craniofacial abnormalities in Six 1 deficient mice. Mech Dev 2003;120:669-79.

10. Ozaki H, Nakamura K, Funahashi J, Ikeda K, Yamada G, Tokano H, Okamura HO, Kitamura K, Muto S, Kotaki H, Sudo K, Horai R, et al. Six1 controls patterning of the mouse otic vesicle. Development (Cambridge, England) 2004;131:551-62.

11. Zheng W, Huang L, Wei ZB, Silvius D, Tang B, Xu PX. The role of Six1 in mammalian auditory system development. Development (Cambridge, England) 2003;130:3989-4000.

12. Relaix F, Buckingham M. From insect eye to vertebrate muscle: redeployment of a regulatory network. Genes & development 1999;13:3171-8.

13. Yu Y, Khan J, Khanna C, Helman L, Meltzer PS, Merlino G. Expression profiling identifies the cytoskeletal organizer ezrin and the developmental homeoprotein Six-1 as key metastatic regulators. Nature medicine 2004;10:175-81.

14. Li CM, Guo M, Borczuk A, Powell CA, Wei M, Thaker HM, Friedman R, Klein U, Tycko B. Gene expression in Wilms' tumor mimics the earliest committed stage in the metanephric mesenchymal-epithelial transition. Am J Pathol 2002;160:2181-90.

15. Ford HL, Kabingu EN, Bump EA, Mutter GL, Pardee AB. Abrogation of the G2 cell

cycle checkpoint associated with overexpression of HSIX1: a possible mechanism of breast carcinogenesis. Proceedings of the National Academy of Sciences of the United States of America 1998;95:12608-13.

16. Behbakht K, Qamar L, Aldridge CS, Coletta RD, Davidson SA, Thorburn A, Ford HL. Six1 overexpression in ovarian carcinoma causes resistance to TRAIL-mediated apoptosis and is associated with poor survival. Cancer Res 2007;67:3036-42.

17. Coletta RD, Christensen K, Reichenberger KJ, Lamb J, Micomonaco D, Huang L, Wolf DM, Muller-Tidow C, Golub TR, Kawakami K, Ford HL. The Six1 homeoprotein stimulates tumorigenesis by reactivation of cyclin A1. Proc Natl Acad Sci U S A 2004;101:6478-83.

18. Li Y, Tang ZY, Ye SL, Liu YK, Chen J, Xue Q, Chen J, Gao DM, Bao WH. Establishment of cell clones with different metastatic potential from the metastatic hepatocellular carcinoma cell line MHCC97. World J Gastroenterol 2001;7:630-6.

19. Sellaro TL, Ravindra AK, Stolz DB, Badylak SF. Maintenance of hepatic sinusoidal endothelial cell phenotype in vitro using organ-specific extracellular matrix scaffolds. Tissue Eng 2007;13:2301-10.

20. Lee TK, Man K, Ho JW, Wang XH, Poon RT, Xu Y, Ng KT, Chu AC, Sun CK, Ng IO, Sun HC, Tang ZY, et al. FTY720: a promising agent for treatment of metastatic hepatocellular carcinoma. Clin Cancer Res 2005;11:8458-66.

21. Li Y, Tang ZY, Ye SL, Liu YK, Chen J, Xue Q, Gao DM, Bao WH. Establishment of cell clones with different metastatic potential from the metastatic hepatocellular carcinoma cell line MHCC97. World J Gastroenterol 2001;7:630-6.

22. Korn WM. Moving toward an understanding of the metastatic process in hepatocellular carcinoma. World J Gastroenterol 2001;7:777-8.

23. Budhu AS, Zipser B, Forgues M, Ye QH, Sun Z, Wang XW. The molecular signature of metastases of human hepatocellular carcinoma. Oncology 2005;69 Suppl 1:23-7.

24. Christensen KL, Patrick AN, McCoy EL, Ford HL. The six family of homeobox genes in development and cancer. Adv Cancer Res 2008;101:93-126.

25. Yu Y, Davicioni E, Triche TJ, Merlino G. The homeoprotein six1 transcriptionally activates multiple protumorigenic genes but requires ezrin to promote metastasis. Cancer Res 2006;66:1982-9.

26. Iizuka N, Tsunedomi R, Tamesa T, Okada T, Sakamoto K, Hamaguchi T, Yamada-Okabe H, Miyamoto T, Uchimura S, Hamamoto Y, Oka M. Involvement of c-myc-regulated genes in hepatocellular carcinoma related to genotype-C hepatitis B virus. J Cancer Res Clin Oncol 2006;132:473-81.

27. Kinugasa N, Higashi T, Nouso K, Nakatsukasa H, Kobayashi Y, Ishizaki M, Toshikuni N, Yoshida K, Uematsu S, Tsuji T. Expression of membrane cofactor protein (MCP, CD46) in human liver diseases. Br J Cancer 1999;80:1820-5.

28. Rodrigues SP, Fathers KE, Chan G, Zuo D, Halwani F, Meterissian S, Park M. CrkI and CrkII function as key signaling integrators for migration and invasion of cancer cells. Mol Cancer Res 2005;3:183-94.

29. Moss ML, Stoeck A, Yan W, Dempsey PJ. ADAM10 as a target for anti-cancer therapy. Curr Pharm Biotechnol 2008;9:2-8.

TABLE I - LIST OF PRIMERS FOR SYBR GREEN REAL-TIME sqRT-PCR

Gene	Forward primer	Reverse primer	Size
ADAM10	5' GCAACATCTGGGGACAAACT 3'	5' TGGCCAGATTCAACAAAACA 3'	110 bp
ADRCE1	5' AATGGTGAAGAAGGCACGTC 3'	5'GCTCTCCGAGCCAGTGTTAC 3'	108 bp
ATF3	5' TCTAGGCTGGAAGAGCCAAA 3'	5' CTGGTACCACCAGCTCCACT 3'	104 bp
CAMK2N1	5' GATTCTTGTATGGCCAGGA 3'	5' GTGGATTCTGCCTCACC 3'	109 bp
CD46	5' CGAGTGTCCCTTTCCTTCCT 3'	5' AAATGTTGGTGGCTCCTCAC 3'	103 bp
CGIP39	5' CTGAGGTCCCTAGCTCGTTG 3'	5' GGGGTCATCCACTCTTGAAA 3'	103 bp
CHAC1	5' CCTCGATCCTCTGCTCACTC 3'	5' TACAGGGCTCCTTCTCCTCA 3'	114 bp
COM1	5' AAAGGTCGCACCAAGAGAGA 3'	5' CCTCGCTTCTTCCTCTCTGA 3'	110 bp
CRKII	5' CCAATGCCTACGACAAGACA 3'	5' ACCTCGTTTGCCATTACACC 3'	110 bp
CTH	5' TGAATGGCCACAGTGATGTT 3'	5' GGAGATGGAACTGCTCCAAG 3'	108 bp
DDIT3	5' CAGAGCTGGAACCTGAGGAG 3'	5' CCATCTCTGCAGTTGGATCA 3'	108 bp
DNAJ9B	5' AATGGCTACTCCCCAGTCAA 3'	5' CCGATTTTGGCACACCTAAG 3'	110 bp
DNMT3B	5' CAAGACTCGAAGACGCACAG 3'	5' ATCTTCATCCCCTCGGTCTT 3'	112 bp
EIF1AX	5' CGCAGGGGTAAGAATGAGAA 3'	5' TTGCTTCTAGCCGTCCATTT 3'	112 bp
Inhibin BE	5' AGGGTAAGGGCTGTTGAGGT 3'	5' TGCCTCATTTTCCTGACTCC 3'	111 bp
MAPKAP	5' TTTCATGCTGGCATTTTTCA 3'	5' CCGCAGATAGCACCATACCT 3'	105 bp
MEIS2e	5' TGAGCAAGGGGATGGTTTAG 3'	5' ACTTTGGGGAAAATGCCTCT 3'	111 bp
NUPL1	5' TTTTCAAACTGGGGAAAACG 3'	5' TTTCCATGATCACCCCAAAT 3'	109 bp
PELI1	5' CCAAATGGCGATAGAGGAAG 3'	5' GCAGCCTGAGGAGTACAAGC 3'	110 bp
PGRMC1	5' GCCTGGATAAGGAAGCACTG 3'	5' GCCCACGTGATGATACTTGA 3'	119 bp
POLR3K	5' CAAGTGCTGCAATGCTCAGT 3'	5' TGCCAGCTAAGCATCTACCC 3'	110 bp
PPP1R15A	5' GAGGAGGCTGAAGACAGTGG 3'	5' ATGCCATCATCATCATCCAA 3'	110 bp
RDH11	5' GCAAGCTAGCCAACATCCTC 3'	5' GTGCCGAACCAGTTCAGATT 3'	113 bp
SESN2	5' TACTTGCCATTCACCCATCA 3'	5' GAACTAGGATTCGGGCAACA 3'	114 bp
SLC4A4	5' TCATGGATCGTCTGAAGCTG 3'	5' CACCTGCAGGAAAGTGAACA 3'	110 bp
STC2	5' GGACAGAACCAAGCTCTCCA 3'	5' CTCTTGCTACCTCGCTCACC 3'	111 bp
TARDBP	5' TACTCCCCCTACCCCTTTGT 3'	5' GTTCTCAGCCCATCAGCTTC 3'	110 bp
TIEG2	5' GCCGAATCCATACACAAGGT 3'	5' GTAAACCATCCCCCTTCCAC 3'	110 bp
YWHAH	5' GACCAGCAGGATGAAGAAGC 3'	5' TTGTGGCAAGGAAGAATCG 3'	107 bp
ZBTB43	5' CCAGATGTGGCATGTGGTAG 3'	5' TACTGCTGCTTGGTGACTGG 3'	110 bp

TABLE II - SUMMARY OF XENOGRAFT METASTASIS MODELS

	MHCC97L-Control	MHCC97L-shSix1	*P* value[a]
Experimental metastasis model			
Liver metastasis	0/7 (0%)	0/8 (0%)	NS
Pulmonary metastasis	3/7 (42.9%)	0/8 (0%)	NS
Spontaneous metastasis model			
Liver tumor formed	8/8 (100%)	6/8 (75%)	NS
Tumor volume (cm^3)	1.84 ± 1.032	0.049 ± 0.014	0.000
Pulmonary metastasis	5/8 (62.5%)	0/8 (0%)	0.026

Note: [a]NS, no significance.

TABLE III - SUMMARY OF DOWN-REGULATED GENES IN MHCC97L-shSix1

Accession	Gene name	Fold change (Microarray)	Fold change[a] (sqRT-PCR)	Functions
NM_003405	Tyrosine 3-monooxygenase-tryptophan 5-monooxygenase activation protein, eta polypeptide (YWHAH)	-2.14	-2.92	Adapter protein implicated in the regulation of a large spectrum of both general and specialized signaling pathways
AB097031	MAPK activating protein (MAPKAP)	-3.35	-2.71	Involved in activation of MAPK signaling pathway
NM_002389	CD46	-2.34	-2.7	A cofactor for complement factor I
BC047523	Calmodulin 1, phosphorylase kinase, delta (CAMK2N1)	-2.3	-2.67	It may mediate the control of a large number of protein kinases and phosphatases
BC034238	Progesterone receptor membrane component 1(PGRMC1)	-2.14	-2.67	A receptor for progesterone
NM_016823	v-crk avian sarcoma virus CT10 oncogene homolog (CRKII)	-2.46	-2.21	Mediates attachment-induced MAPK8 activation, membrane ruffling and cell motility in a Rac-dependent manner.
NM_016310	Polymerase (RNA) III polypeptide K (POLR3K)	-2.14	-2.51	Functions in RNA synthesis
NM_003759	Solute carrier family 4, sodium bicarbonate cotransporter, member 4 (SLC4A4)	-2.14	-2.44	Involved in regulation of intracellular PH
NM_016026	Retinol dehydrogenase 11 (RDH11)	-2	-2.44	Exhibits an oxidoreductive catalytic activity towards retinoid
NM_001110	ADAM metallopeptidase domain 10 (ADAM10)	-2	-2.42	Responsible for the proteolytic release of several cell-surface proteins
NM_020651	Pellino homolog 1 (PELI1)	-2.14	-2.21	Scaffold protein involved in the IL-1 signaling pathway
BC069196	SWI/SNF related, matrix associated, actin dependent regulator of chromatin, subfamily e, member 1 (ADRCE1)	-2.46	-2.12	Involved in transcriptional activation and repression of select genes by chromatin remodeling
NM_020149.1	TALE homeobox protein Meis2e (MEIS2E)	-2	-2.0	A transcriptional factor
AL079283.1	Eukaryotic translation initiation factor 1A, X-linked (EIF1AX)	-2.64	-2.08	Involved in maximization of the rate of protein biosynthesis
NM_007375.1	TAR DNA binding protein (TARDBP)	-2	-2	Involved in the regulation of CFTR splicing
NM_006667.2	Progesterone binding protein	-2.14	UC	A putative steroid membrane receptor
NM_006827	Transmembrane emp24-like trafficking protein 10	-2	UC	Involved in vesicular protein trafficking
U07802	Butyrate response factor 2 (EGF-response factor 2)	-2	UC	A putative nuclear transcription factor most likely functions in regulating the response to growth factors
AI346910	VAMP (vesicle-associated membrane protein)-associated protein A	-2	UC	Functions in vesicle trafficking, membrane fusion, protein complex assembly and cell motility
AA885297	CD36 antigen (collagen type I receptor, thrombospondin receptor)-like 2	-2.3	UC	Participates in membrane transportation and the reorganization of endosomal/lysosomal compartment
BF246917	Protein kinase, cAMP-dependent, regulatory, type II, alpha (PRKAR2A)	-2.14	UC	Regulates protein transport from endosomes to the Golgi apparatus and further to the endoplasmic reticulum (ER)
AV725664	Phosphatidic acid phosphatase type 2B (PPAP2B)	-2	UC	Actively hydrolyzes extracellular lysophosphatidic acid and short-chain phosphatidic acid
NM_006375.1	Cytosolic ovarian carcinoma antigen 1 (COVA1)	-2	UC	The encoded protein has two enzymatic activities: catalysis of hydroquinone or NADH oxidation, and protein disulfide interchange
AW195360	Integral inner nuclear membrane protein	-2	UC	A membrane protein
BF692332	Ribosomal protein S4, X-linked	-2.3	UC	Catalyzes protein synthesis
L11372.1	Protocadherin 43	-2	UC	Plays a critical role in the establishment and function of specific cell-cell connections in the brain
BF061658	Transforming growth factor, beta 2(TGFB2)	-2	UC	Plays a role in regulation of cell growth and proliferation and may be involved in mesenchymal-epithelial cell interactions during development
AW022607	Glyceronephosphate O-acyltransferase	-2	UC	Catalyzes the transesterification of dihydroxyacetone phosphate (DHAP) to form acyl-DHAP

Note: [a]UC, un-confirmed by sqRT-PCR.

TABLE IV - SUMMARY OF UP-REGULATED GENES IN MHCC97L-shSix1

Accession	Gene name	Fold change (Microarray)	Fold change[a] (sqRT-PCR)	Functions
AF288391.1	Cell growth inhibiting protein 39	4.59	8.94	Related to growth inhibition
BC005161.1	Inhibin BE	4.59	5.27	Inhibits the secretion of follitropin by the pituitary gland.
NM_001902.1	Cystathionase (cystathionine gamma-lyase) (CTH)	2.64	4.9	Functions in amino-acid biosynthesis
NM_024111.1	ChaC, cation transport regulator homolog 1(CHAC1)	3.48	4.848	Cation transport regulator
BC000658.1	Stanniocalcin 2 (STC2)	2.14	4.32	Anti-hypocalcemic action on calcium and phosphate homeostasis
AB066566.1	ATF3 mRNA for activating transcription factor 3 delta Zip2 (ATF3)	3.25	4.31	Represses transcription from promoters with ATF sites
BF131886	Sestrin 2 (SESN2)	3.03	4.132	Involved in regulation of cell growth and survival
AF135266.1	p8 protein homolog (COM1)	2.30	3.98	A structure protein
NM_012328.1	DnaJ (Hsp40) homolog, subfamily B, member 9 (DNAJB9)	2.3	3.90	A co-chaperone with Hsp70 protein
NM_014778.1	Nucleoporin like 1 (NUPL1)	2.64	3.84	Involved in regulation of protein trafficking
BC003637.1	DNA-damage-inducible transcript 3 (DDIT3)	2.14	3.81	Negative regulator of transcriptional factors
NM_006892.1	DNA (cytosine-5-)-methyltransferase 3 beta (DNMT3B)	2.64	3.32	Involved in DNA methylation and development
AA149594	TGFB inducible early growth response 2 (TIEG-2)	2	3.05	A transcriptional factor
NM_014007.1	Zinc finger and BTB domain containing 43 (ZBTB43)	2.14	2.86	Involved in transcriptional regulation
NM_014330.2	Protein phosphatase 1, regulatory inhibitor subunit 15A (PPP1R15A)	2	2.60	A growth arrest and DNA-damage-inducible protein
M57731.1	Cytokine gro-beta	2	UC	Cytokine
NM_000565.1	Interleukin 6 receptor (IL6R)	3.03	UC	Potent pleiotropic cytokine that regulates cell growth and differentiation and plays an important role in immune response
M27968.1	Fibroblast growth factor 2	2	UC	Implicated in diverse biological processes, such as limb and nervous system development, wound healing, and tumor growth
AB052156.1	MAPK phosphatase-7	2.14	UC	Negatively regulates MAPK activity
AF202640.1	Orphan G-protein coupled receptor (GPRC5B)	2	UC	Mediates the cellular effects of retinoic acid on the G protein signal transduction cascade
J03580.1	Parathyroid hormone-like hormone	2.64	UC	Regulates endochondral bone development and epithelial-mesenchymal interactions during the formation of the mammary glands and teeth
AI268381	Regulatory solute carrier protein, family 1	2	UC	Membrane-associated modulator of the sodium-glucose cotransport system
AF031587.1	MIP-1 delta	2	UC	Induces changes in intracellular calcium concentration in monocytes and is thought to act through the CCR1 receptor
NM_001561.2	Tumor necrosis factor receptor superfamily, member 9 (TNFRSF9)	4	UC	Contributes to the clonal expansion, survival, and development of T cells

Note: [a]UC, un-confirmed by sqRT-PCR

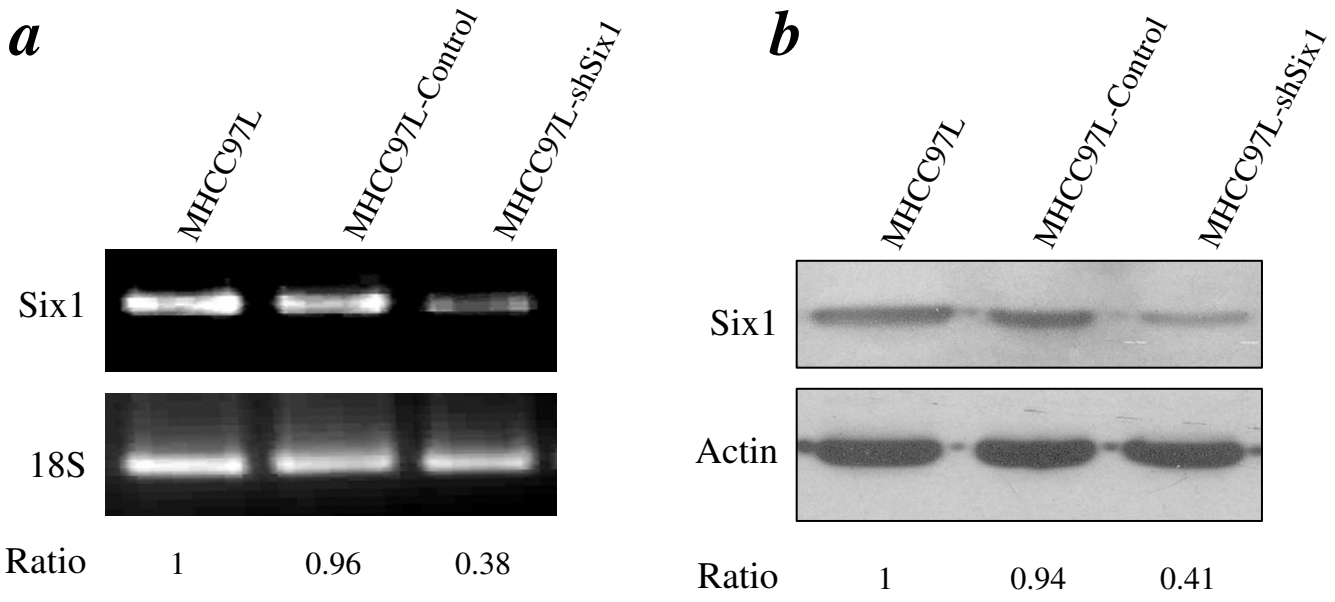

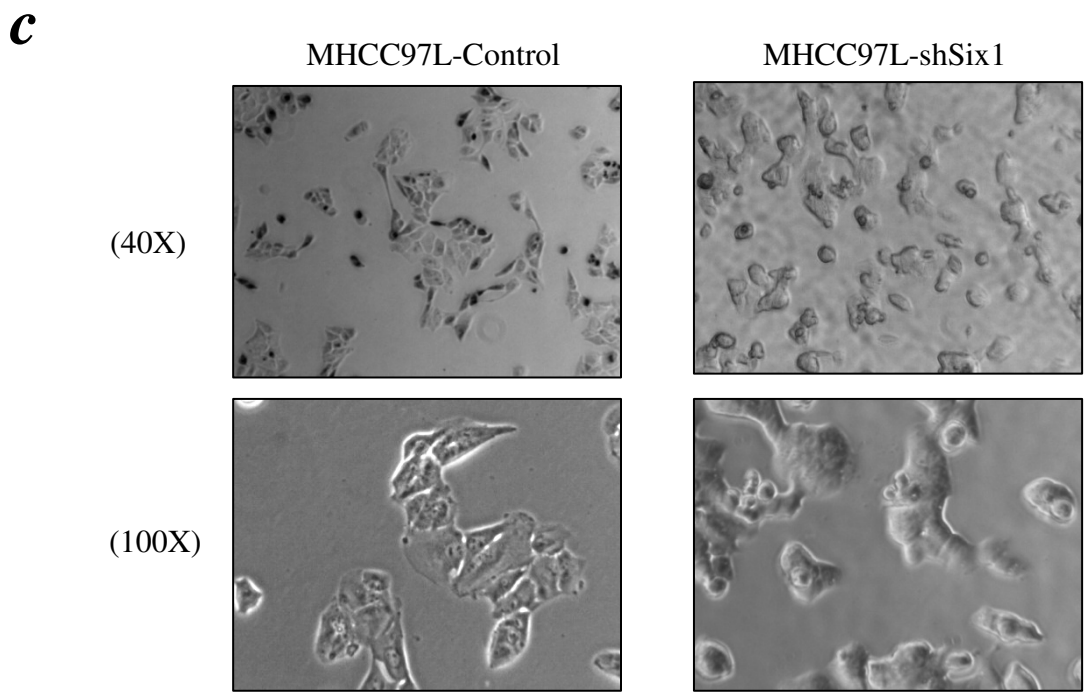

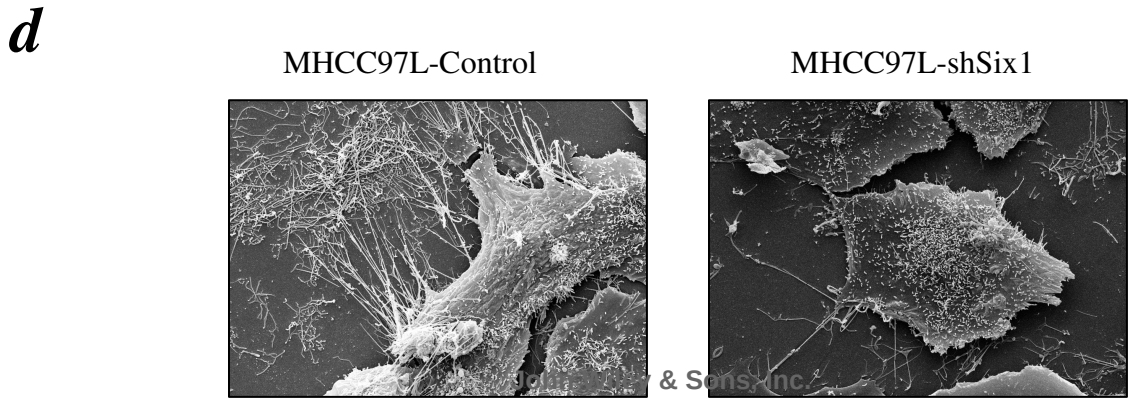

FIGURE 1

a

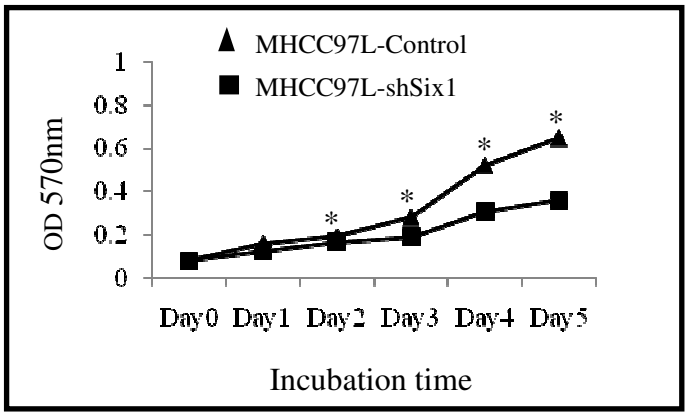
MHCC97L-Control
MHCC97L-shSix1
OD 570nm
1
0.8
0.6
0.4
0.2
0
*
*
*
*
Day0 Day1 Day2 Day3 Day4 Day5
Incubation time

b

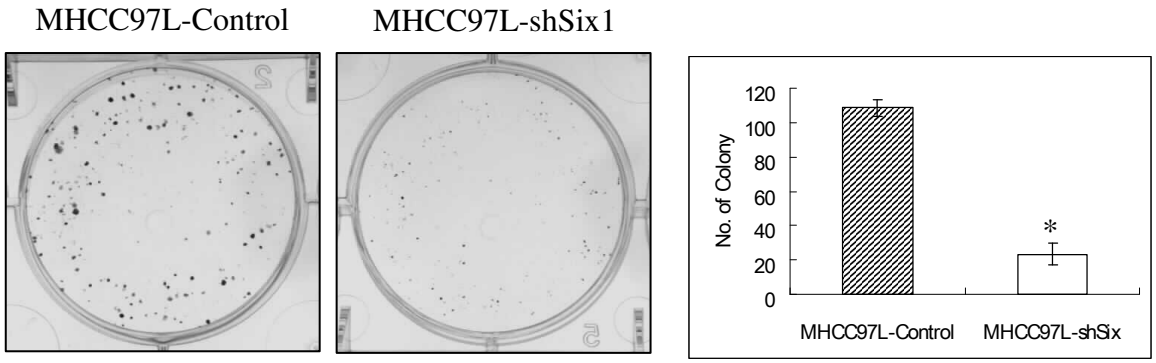
MHCC97L-Control
MHCC97L-shSix1
No. of Colony
120
100
80
60
40
20
0
*
MHCC97L-Control
MHCC97L-shSix

FIGURE 2

a

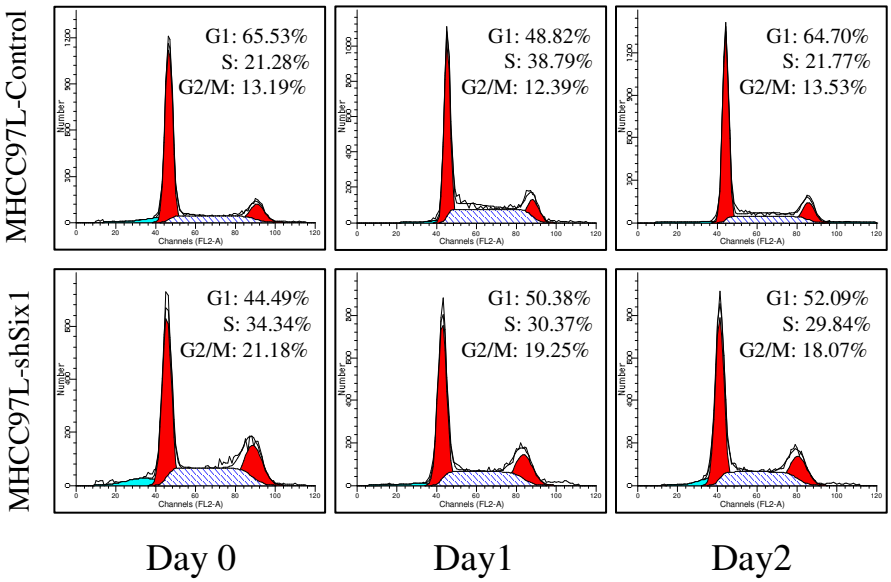
MHCC97L-Control
MHCC97L-shSix1
G1: 65.53%
S: 21.28%
G2/M: 13.19%
G1: 48.82%
S: 38.79%
G2/M: 12.39%
G1: 64.70%
S: 21.77%
G2/M: 13.53%
G1: 44.49%
S: 34.34%
G2/M: 21.18%
G1: 50.38%
S: 30.37%
G2/M: 19.25%
G1: 52.09%
S: 29.84%
G2/M: 18.07%
Number
Channels (FL2-A)
Day 0
Day1
Day2

b

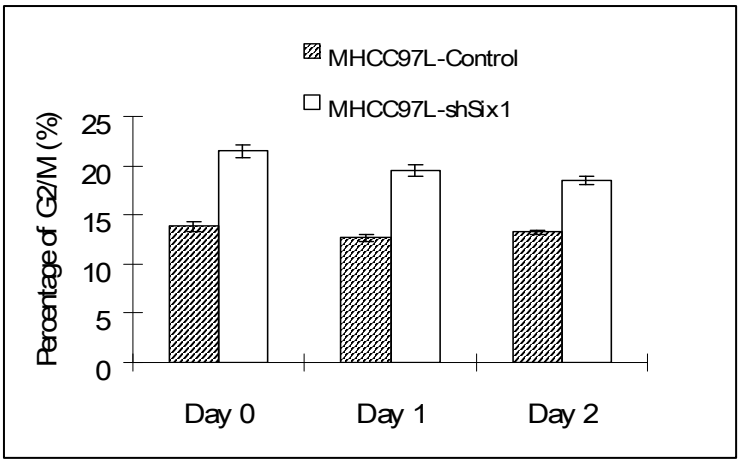
MHCC97L-Control
MHCC97L-shSix1
Percentage of G2/M (%)
25
20
15
10
5
0
Day 0
Day 1
Day 2

FIGURE 3

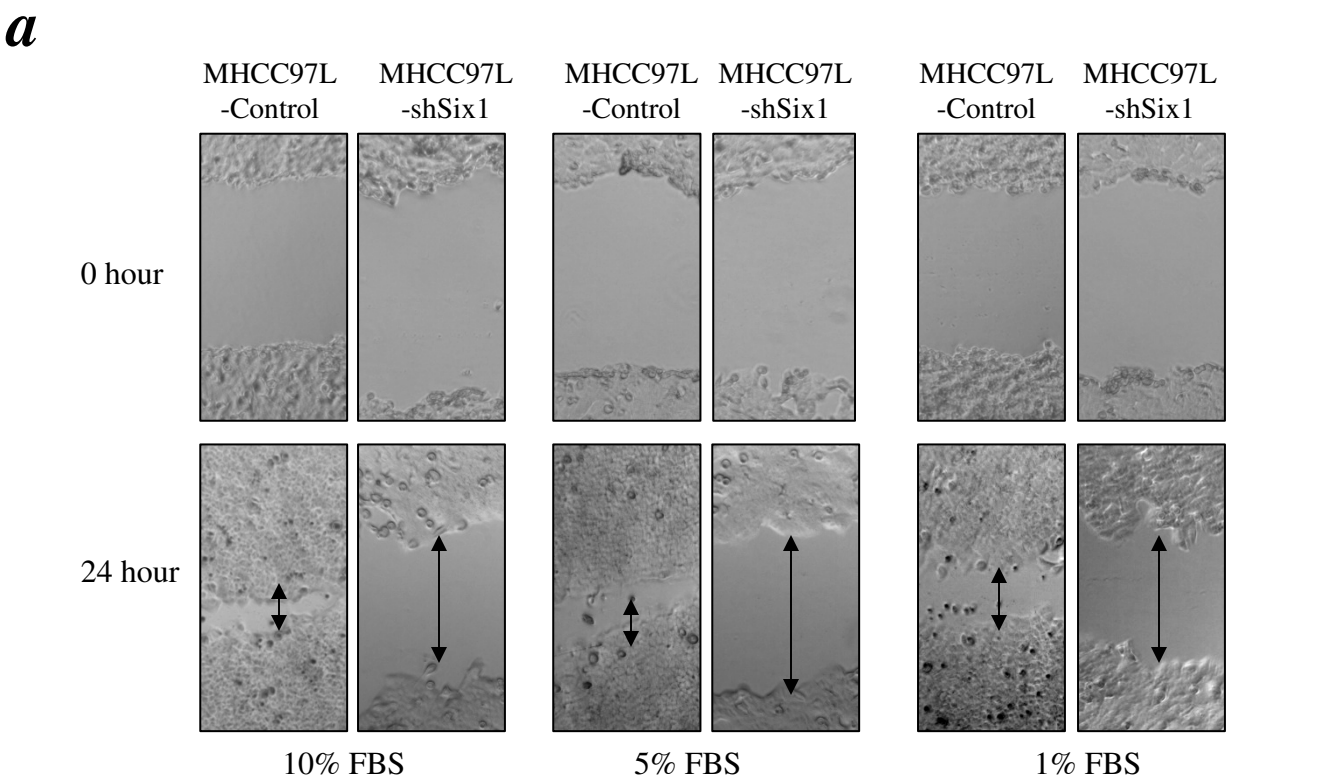
a
MHCC97L -Control
MHCC97L -shSix1
MHCC97L -Control
MHCC97L -shSix1
MHCC97L -Control
MHCC97L -shSix1
0 hour
24 hour
10% FBS
5% FBS
1% FBS

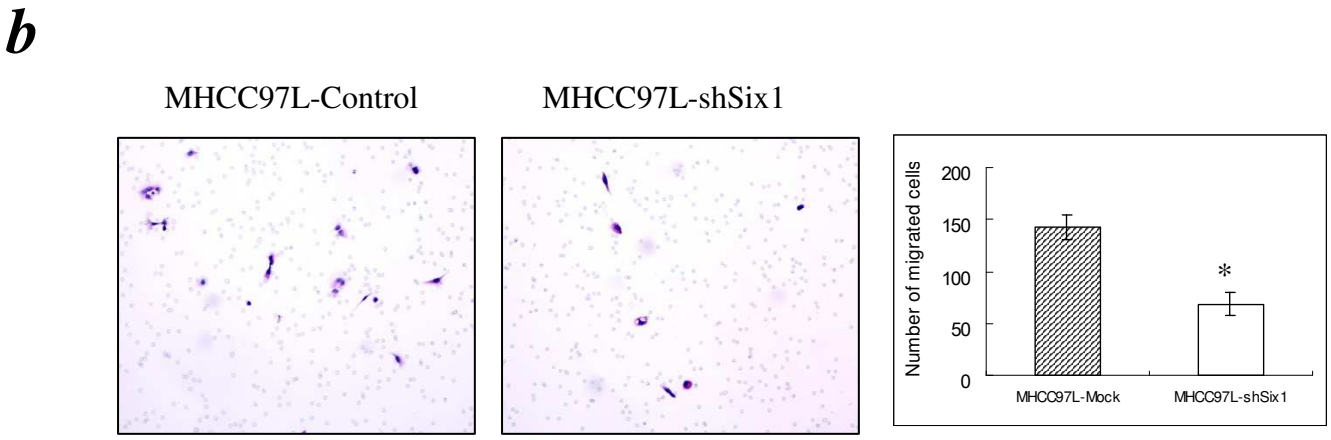
b
MHCC97L-Control
MHCC97L-shSix1
Number of migrated cells
200
150
100
50
0
*
MHCC97L-Mock
MHCC97L-shSix1

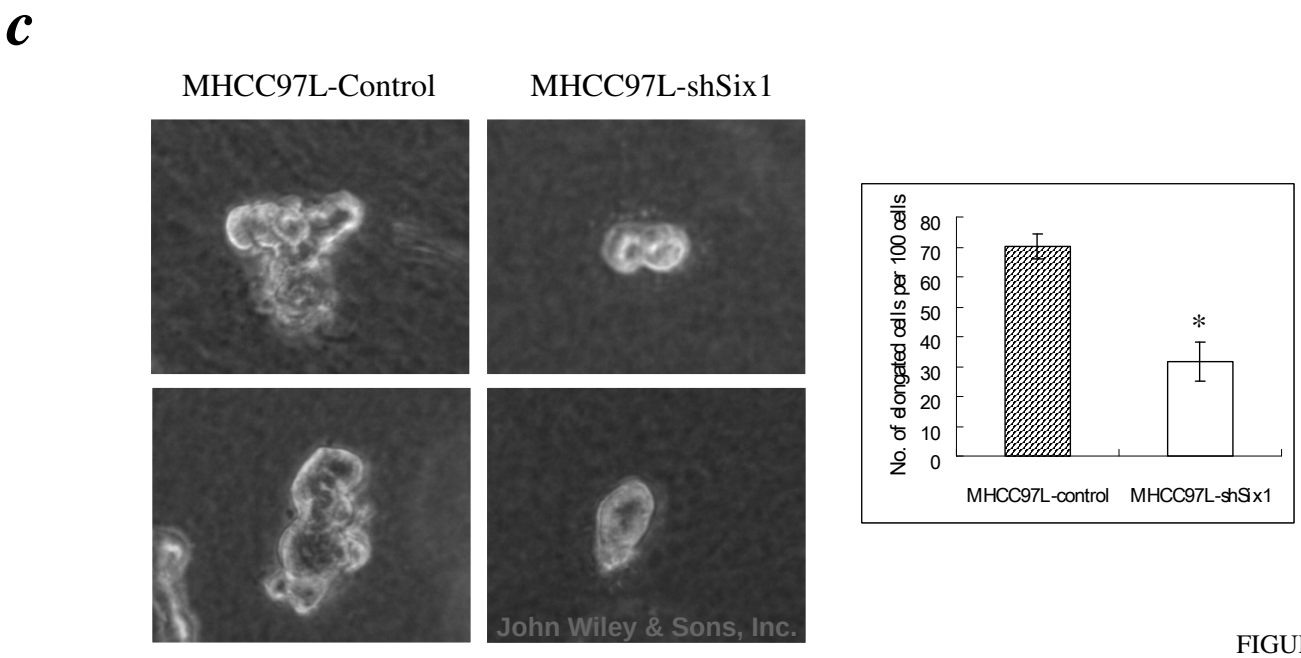
c
MHCC97L-Control
MHCC97L-shSix1
No. of elongated cells per 100 cells
80
70
60
50
40
30
20
10
0
*
MHCC97L-control
MHCC97L-shSix1
John Wiley & Sons, Inc.

FIGURE 4

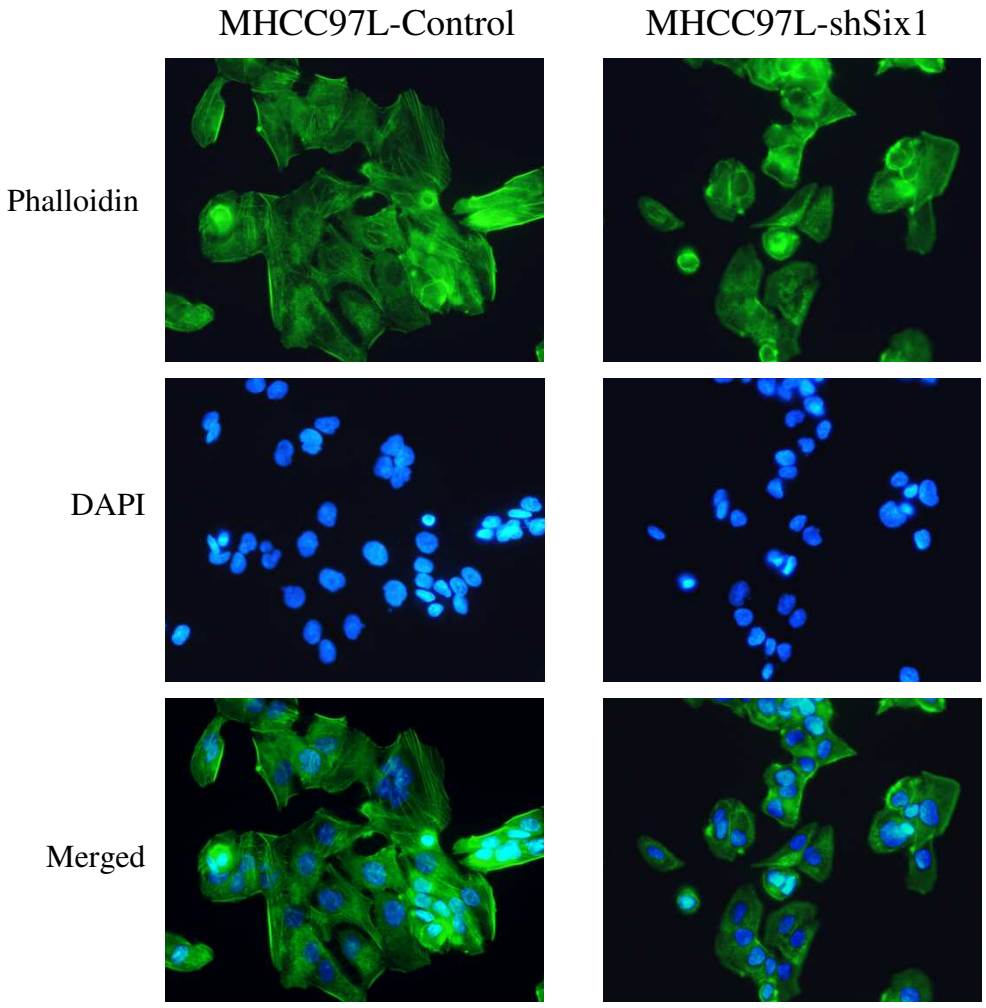

FIGURE 5

a


MHCC97L-Control
MHCC97L-shSix1

b

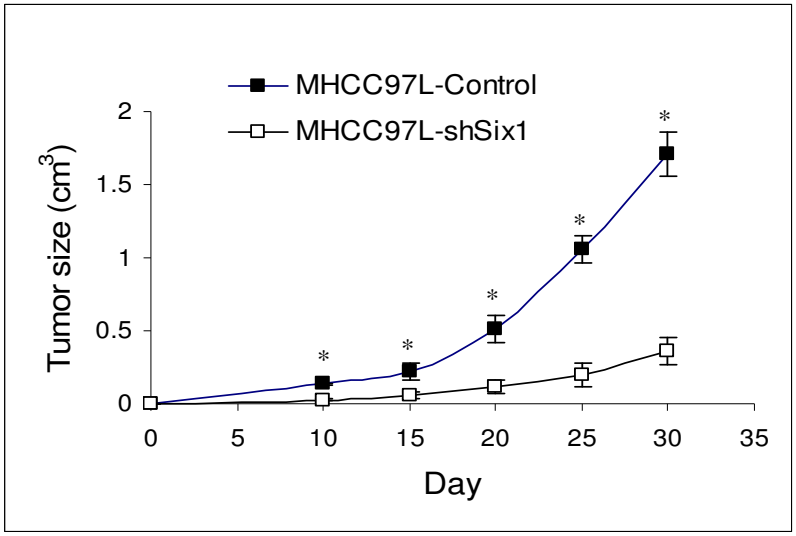
MHCC97L-Control
MHCC97L-shSix1
Tumor size (cm3)
Day
0
0.5
1
1.5
2
0
5
10
15
20
25
30
35
*

c

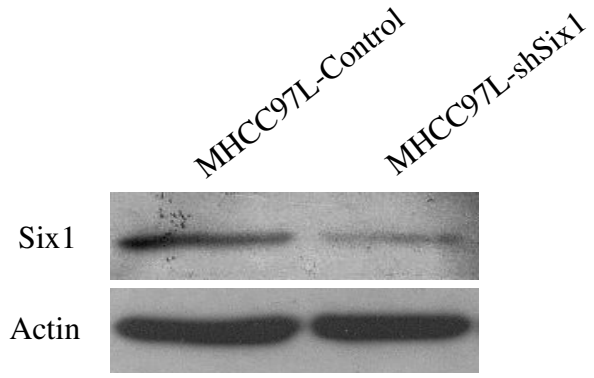
MHCC97L-Control
MHCC97L-shSix1
Six1
Actin

FIGURE 6

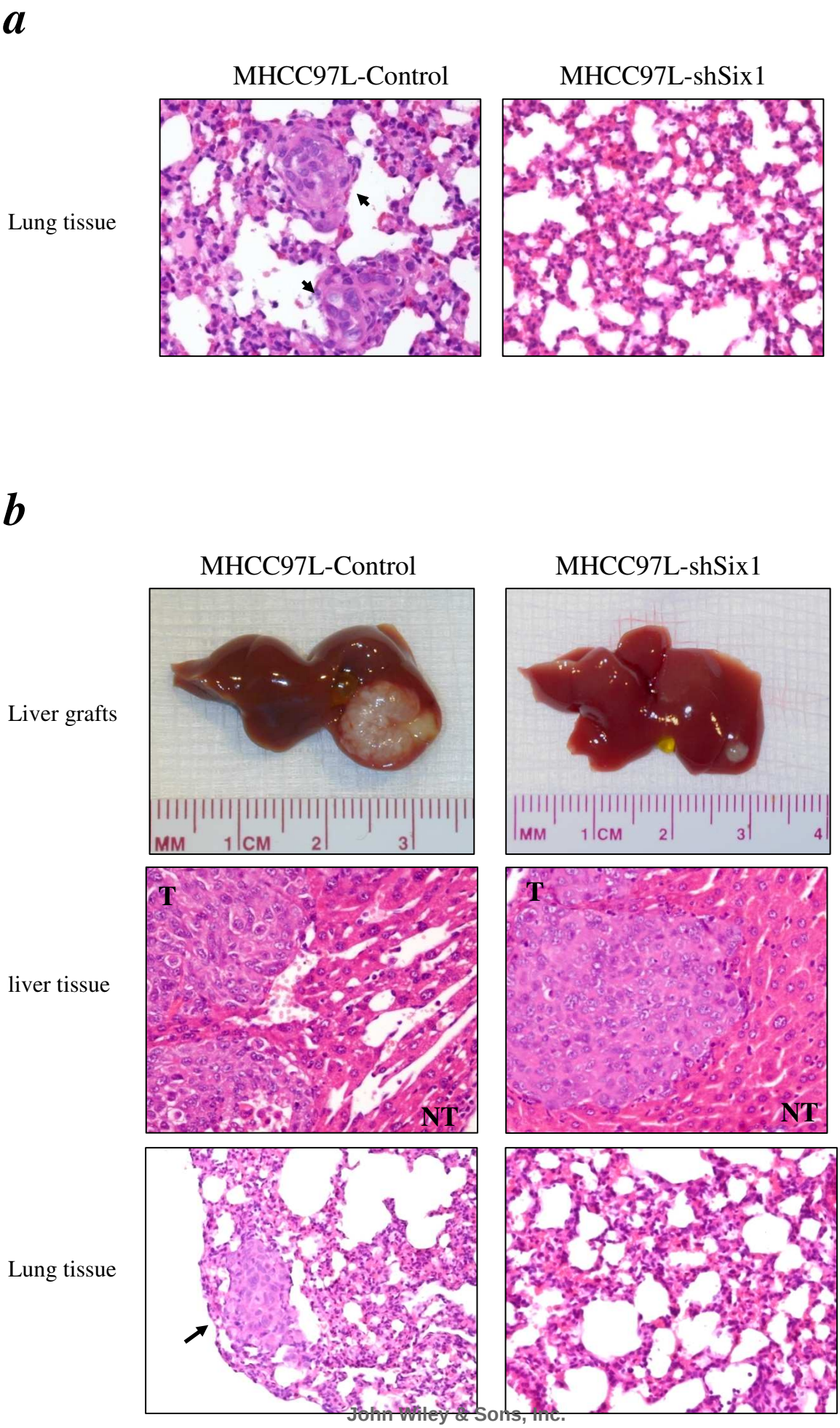

FIGURE 7

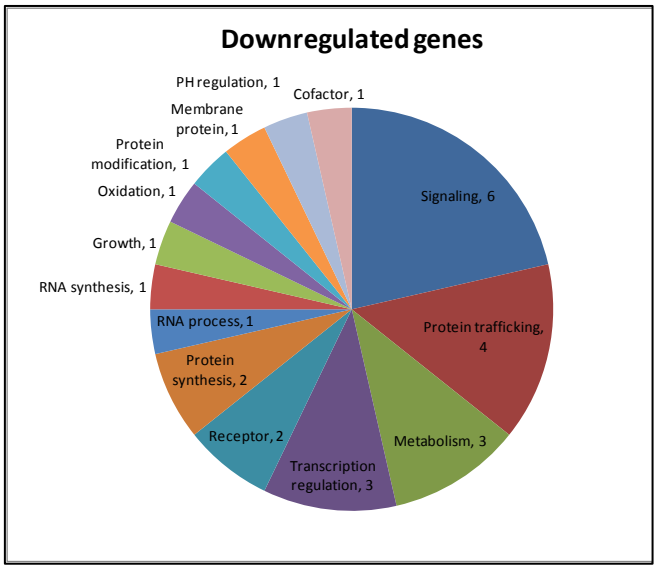
Downregulated genes
PH regulation, 1
Cofactor, 1
Membrane protein, 1
Protein modification, 1
Oxidation, 1
Growth, 1
RNA synthesis, 1
RNA process, 1
Protein synthesis, 2
Receptor, 2
Transcription regulation, 3
Metabolism, 3
Protein trafficking, 4
Signaling, 6

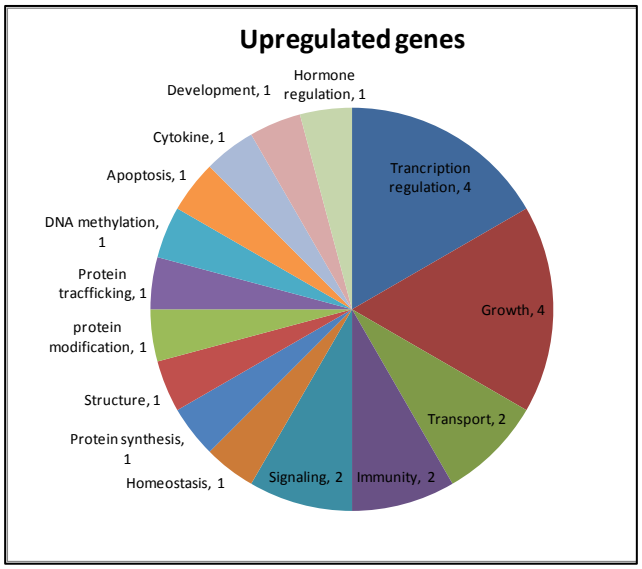
Upregulated genes
Development, 1
Hormone regulation, 1
Cytokine, 1
Apoptosis, 1
DNA methylation, 1
Protein tracfficking, 1
protein modification, 1
Structure, 1
Protein synthesis, 1
Homeostasis, 1
Signaling, 2
Immunity, 2
Transport, 2
Growth, 4
Trancription regulation, 4

FIGURE 8